SLAC-PUB-13064
arXiv:0711.4769v1[hep-ex]

D and D_s hadronic branching fractions at B factories

M. Pappagallo(on behalf of the *BABAR* Collaboration)
University of Bari and I.N.F.N., 70126 Bari, Italy

Recent measurements of hadronic branching fractions of D and D_s mesons, performed by the *BABAR* and Belle experiments at the asymmetric e^+e^- B factories colliders PEP II and KEKB, are reviewed.

1. Introduction

Hadronic branching fractions of D and D_s decays are used as references mode in many measurements of branching fractions of D and B-meson decays as well. A precise measurement of such values improves our knowledge of D and B-meson properties, and of fundamental parameters of the Standard Model, such as the magnitude of the Cabibbo-Kobayashi-Maskawa [1] matrix element.

2. Absolute branching fraction of $\mathbf{D^0 \to K^-\pi^+}$

BABAR collaboration measures the absolute branching fraction $\mathcal{B}(D^0 \to K^-\pi^+)$[1] using $D^0 \to K^-\pi^+$ decays in a sample of D^0 mesons preselected by their production in D^{*+} decays, obtained with partial reconstruction of the decay $\overline{B}^0 \to D^{*+}X\ell^-\bar{\nu}_\ell$, with $D^{*+} \to D^0\pi^+$ [2]. Such measurement is extremely important because many of the past and current D and B branching fraction measurements are indeed systematically limited by the precision of $\mathcal{B}(D^0 \to K^-\pi^+)$.

A sample of partially reconstructed B mesons in the channel $\overline{B}^0 \to D^{*+}X\ell^-\bar{\nu}_\ell$ is selected by retaining events containing a charged lepton ($\ell = e, \mu$) and a low momentum pion (soft pion, π_s^+) which may arise from the decay $D^{*+} \to D^0\pi_s^+$. This sample of events is referred to as the "inclusive sample".

Using conservation of momentum and energy, the invariant mass squared of the undetected neutrino is calculated as

$$\mathcal{M}_\nu^2 \equiv (E_{\rm beam} - E_{D^*} - E_\ell)^2 - (\vec{p}_{D^*} + \vec{p}_\ell)^2,$$

where $E_{\rm beam}$ is half the total center-of-mass energy, E_ℓ (E_{D^*}), $\vec{p}_\ell$ ($\vec{p}_{D^*}$) are the energy and momentum of the lepton (the D^* meson) and the magnitude of the B meson momentum, p_B, is considered negligible compared to p_ℓ and p_{D^*}. Figure 1 shows the $\mathcal{M}_\nu^2$ distribution and the results of a minimum χ^2 fit aiming to determine the signal and background contribution.

[1]Charge conjugation is implied through the paper.

The number of signal events with $\mathcal{M}_\nu^2 > -2$ GeV^2/c^4 results $N^{\rm incl} = (2170.64 \pm 3.04({\rm stat}) \pm 18.1({\rm syst})) \times 10^3$.

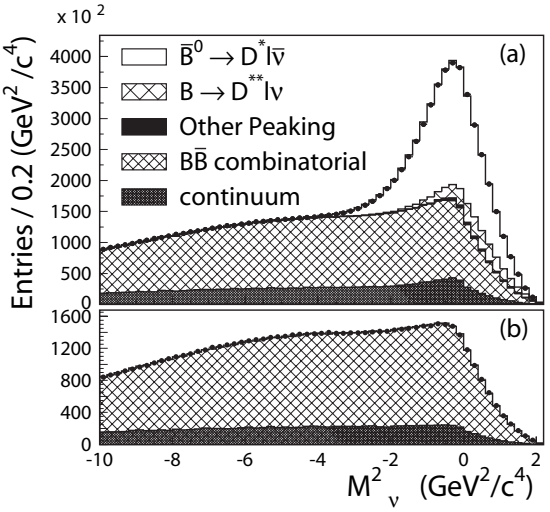

Figure 1: The $\mathcal{M}_\nu^2$ distribution of the inclusive sample, for right-charge (a) and wrong-charge (b) samples. The data are represented by solid points with error. The MC fit results are overlaid to the data, as explained in the figure.

The $D^0 \to K^-\pi^+$ decays in the inclusive sample are selected requiring events in the mass range $1.82 < M_{K\pi} < 1.91$ GeV/c^2 and $142.4 < \Delta M < 149.9$ MeV/c^2 where $\Delta M = M(K^-\pi^+\pi_s^+) - M(K^-\pi^+)$ and π_s^+ is the slow pion from D^{*+} decay. The exclusive selection yields $N^{\rm excl} = 33810 \pm 290$ signal events, where the error is statistical only.

The branching fraction is computed as

$$\mathcal{B}(D^0 \to K^-\pi^+) = \frac{N^{\rm excl}}{N^{\rm incl}} \frac{1}{\varepsilon_{(K^-\pi^+)}\zeta},$$

where $\varepsilon_{(K^-\pi^+)}$ is the D^0 reconstruction efficiency as computed in the simulation, and ζ is the selection bias introduced by the partial reconstruction.

The main systematic uncertainty on $N^{\rm incl}$ and $N^{\rm excl}$ are respectively due to the non-peaking combinatorial $B\overline{B}$ background and the charged-track reconstruction efficiency. The complete set of systematic uncertainties is listed in Tab. I. The absolute branching fraction of $D^0 \to K^-\pi^+$ decay results

$$\mathcal{B}(D^0 \to K^-\pi^+) = (4.007 \pm 0.037 \pm 0.070)\%,$$

Contributed to International Workshop on Charm Physics (Charm 2007), 8/5/2007-8/8/2007, Ithaca, NY, USA
Work supported in part by US Department of Energy contract DE-AC02-76SF00515

where the first error is statistical and the second error is systematic. This result is comparable in precision with the present world average, and it is consistent with it within two standard deviations.

Table I The relative systematic errors of $\mathcal{B}(D^0 \to K^-\pi^+)$.

	Source	$\delta(\mathcal{B})/\mathcal{B}(\%)$
	Selection bias	± 0.35
$N^{\rm incl}$	Non-peaking combinatorial background	± 0.89
	Peaking combinatorial background	± 0.34
	Soft pion decays in flight	± 0.10
	Fake leptons	± 0.08
	Cascade decays	± 0.08
	Monte Carlo events shape	± 0.08
	Continuum background	± 0.05
	D^{**} production	± 0.02
	Photon radiation	± 0.02
$N^{\rm excl}$	Tracking efficiency	± 1.00
	K^- identification	± 0.70
	D^0 invariant mass	± 0.56
	Combinatorial background shape	± 0.30
	Combinatorial background normalization	± 0.16
	Soft pion decay	± 0.12
	Cabibbo-suppressed decays	± 0.10
	Photon radiation in D^0 decay	± 0.07
Total		± 1.74

3. Absolute branching fraction of $\mathbf{D_s^+ \to K^+K^-\pi^+}$

The poor accuracy of the branching fraction $\mathcal{B}(D_s^+ \to K^+K^-\pi^+) = (5.2 \pm 0.9)\%$ [3] has been a systematic limitation for some precise measurements. In particular, the recent study of the CP violation in $B^0 \to D^{(*)\pm}\pi^{\mp}$ decays is restricted by the knowledge of the ratio of two amplitudes that determine the CP-asymmetry [4, 5]. The amplitude $B^0 \to D^{(*)+}\pi^-$ can be calculated from the branching fraction of $B^0 \to D_s^{(*)+}\pi^-$ decays assuming factorization. On the other hand, the factorization hypothesis can be tested by measuring the ratio of $B^0 \to D^{(*)-}\pi^+$ and $B^0 \to D^{(*)-}D_s^+$ decays. Both $\mathcal{B}(B^0 \to D_s^{(*)+}\pi^-)$ and $\mathcal{B}(B^0 \to D^{(*)-}D_s^+)$ measurements can be improved with better accuracy in D_s^+ absolute branching fractions.

Belle collaboration measures $\mathcal{B}(D_s^+ \to K^+K^-\pi^+)$ using a partial reconstruction of the process $e^-e^- \to D_s^{*+}D_{s1}^-$ [6]. In this analysis 4-momentum conservation allows to infer the 4-momentum of the undetected part.

The process $e^-e^- \to D_s^{*+}D_{s1}^-$ is reconstructed using two different tagging procedures. The first one (denoted as the D_{s1}^- tag) includes the full reconstruction of the D_{s1}^- meson via $D_{s1}^- \to \overline{D}^*K$ decay and observation of the photon from $D_s^{*+} \to D_s^+\gamma$, while the D_s^+ is not reconstructed. The measured signal yield with the D_{s1}^- tag is proportional to the branching fractions of the reconstructed $\overline{D}^*$ modes. In the second procedure (denoted as the D_s^{*+} tag) a full reconstruction of D_s^{*+} is required through $D_s^{*+} \to D_s^+\gamma$ and observation of the kaon from $D_{s1}^- \to \overline{D}^*K$, but the $\overline{D}^*$ is not reconstructed. Since the D_s^+ meson is reconstructed in the channel of interest, $D_s^+ \to K^+K^-\pi^+$, the signal yield measured with the D_s^{*+} tag is proportional to this D_s^+ branching fraction. The (efficiency-corrected) ratio of the two measured signal yields is equal to the ratio of well-known $\overline{D}^*$ branching fractions and the branching fraction of the D_s^+:

$$\mathcal{B}(D_s^+ \to K^+K^-\pi^+) = \frac{N(D_s^{*+})}{N(D_{s1}^-)} \cdot \frac{\epsilon(D_{s1}^-)}{\epsilon(D_s^{*+})}\mathcal{B}(\overline{D}^{(*)}), \quad (1)$$

where $\mathcal{B}(\overline{D}^{(*)})$ is the product of $\overline{D}^*$ branching fraction and those of sub-decays.

The signal is identified by studying the mass recoiling against the reconstructed particle (or combination of particles) denoted as X. This recoil mass is defined as:

$$M_{\rm recoil}(X) \equiv \sqrt{(E_{CM} - E_X)^2 - P_X^2},$$

where E_X and P_X are the center-of-mass (CM) energy and momentum of X, respectively; E_{CM} is the CM beam energy. A peak in the $M_{\rm recoil}$ distribution at the nominal mass of the recoil particle is expected.

Since the resolution in $M_{\rm recoil}$ is not enough to separate the relevant final states, the recoil mass difference $\Delta M_{\rm recoil}$ is used to disentangle the contribution of the different final states:

$$\Delta M_{\rm recoil}(D_{s1}^-\gamma) \equiv M_{\rm recoil}(D_{s1}^-) - M_{\rm recoil}(D_{s1}^-\gamma),$$

$$\Delta M_{\rm recoil}(D_s^{*+}K) \equiv M_{\rm recoil}(D_s^{*+}) - M_{\rm recoil}(D_s^{*+}K).$$

As the ratio of $D_{s1}^- \to \overline{D}^{*0}K^-$ and $D_{s1}^- \to D^{*-}K_S^0$ branching fractions is unknown, the analysis is performed for these two channels separately. Figure 2 shows the $\Delta M_{\rm recoil}(D_{s1}^-\gamma)$ and $\Delta M_{\rm recoil}(D_s^{*+}K)$ distributions used for D_{s1}^- and D_s^{*+} tag procedures respectively. $\Delta M_{\rm recoil}(D_{s1}^-\gamma)$ peaks at around $\simeq 0.14$ GeV/c$^2 \simeq M(D_s^*) - M(D_s)$. $\Delta M_{\rm recoil}(D_s^{*+}K)$ peaks at around $\simeq 0.525$ GeV/c$^2 \simeq M(D_{s1}) - M(D^*)$.

Using the measured signal yields $N(D_s^{*+})$ and $N(D_{s1}^-)$ with D_s^{*+} and D_{s1}^- tags, respectively, and taking into account the efficiency ratio $\frac{\epsilon(D_{s1}^-)}{\epsilon(D_s^{*+})}$, the D_s^+ absolute branching fraction is computed by Eq. 1 for $D_{s1}^- \to \overline{D}^{*0}K^-$ and $D_{s1}^- \to D^{*-}K_S^0$. The average value is $\mathcal{B}(D_s^+ \to K^+K^-\pi^+) = (4.0 \pm 0.4(\text{stat}) \pm 0.4(\text{syst}))\%$.

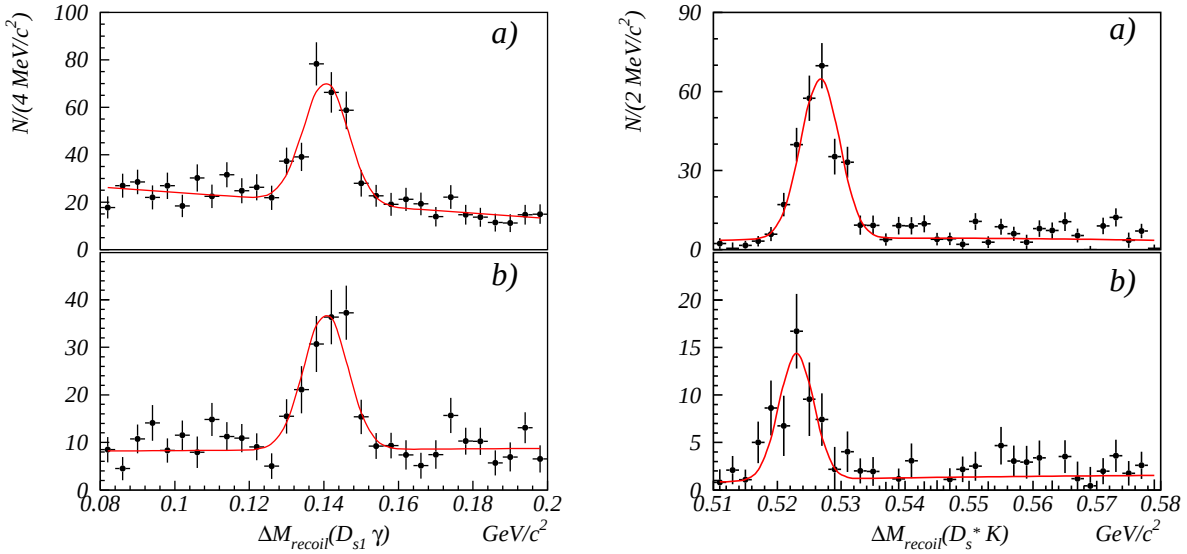

Figure 2: The $e^-e^- \to D_s^{*+}D_{s1}^-$ signal yields in bins of $\Delta M_{\rm recoil}(D_{s1}^-\gamma)$(*left*) and $\Delta M_{\rm recoil}(D_s^{*+}K)$(*right*): a) for the $D_{s1}^- \to \overline{D}^{*0}K^-$ channel and b) for the $D_{s1}^- \to D^{*-}K_S^0$ channel.

4. Relative branching fraction of $D^0 \to K^-K^-\pi^0$ and $D^0 \to \pi^+\pi^-\pi^0$

The branching ratios of the singly Cabibbo-suppressed decays of D^0 meson are anomalous since the $D^0 \to \pi^-\pi^+$ branching fraction is observed to be suppressed relative to the $D^0 \to K^-K^+$ by a factor of almost three, even though the phase space for the former is larger. The branching ratios of the three-body decays [3] have larger uncertainties but do not appear to exhibit the same suppression. This motivates the current study which measures the branching ratios of $D^0 \to \pi^-\pi^+\pi^0$ and $K^-K^+\pi^0$ with respect to the Cabbibo-favored decay $D^0 \to K^-\pi^+\pi^0$. *BABAR* collaboration measures both branching ratios [7], Belle collaboration only the decay $D^0 \to \pi^-\pi^+\pi^0$ with respect to the decay $D^0 \to K^-\pi^+\pi^0$ [8]. By choosing the normalization mode $D^0 \to K^-\pi^+\pi^0$, many sources of systematic uncertainty including the π^0 detection efficiency and uncertainty in the tracking efficiency cancel out. To reduce combinatorial backgrounds, D^0 candidates are reconstructed in decays $D^{*+} \to D^0\pi_s^+$ (π_s^+ is a soft, low momentum charged pion) with $D^0 \to K^-\pi^+\pi^0$, $\pi^-\pi^+\pi^0$, and $K^-K^+\pi^0$, by selecting events with at least three charged tracks and a neutral pion.

BABAR obtains the following results for the branching ratios:

$$\frac{\mathcal{B}(D^0 \to \pi^-\pi^+\pi^0)}{\mathcal{B}(D^0 \to K^-\pi^+\pi^0)} = (10.59 \pm 0.06 \pm 0.13) \times 10^{-2},$$

$$\frac{\mathcal{B}(D^0 \to K^-K^+\pi^0)}{\mathcal{B}(D^0 \to K^-\pi^+\pi^0)} = (2.37 \pm 0.03 \pm 0.04) \times 10^{-2},$$

while Belle obtains:

$$\frac{\mathcal{B}(D^0 \to \pi^+\pi^-\pi^0)}{\mathcal{B}(D^0 \to K^-\pi^+\pi^0)} = (9.71 \pm 0.09 \pm 0.30) \times 10^{-2}.$$

Errors are statistical and systematic, respectively. Figure 3 shows the resulting mass distributions. Reflected $K^-\pi^+\pi^0$ events peak in the lower (upper) sideband of $m_{\pi^-\pi^+\pi^0}$ ($m_{K^-K^+\pi^0}$).

Using the world average value for the $D^0 \to K^-\pi^+\pi^0$ branching fraction [3], the absolute branching ratios result:

BABAR

$$\mathcal{B}(D^0 \to \pi^-\pi^+\pi^0) = (1.493 \pm 0.008 \pm 0.018 \pm 0.053)\%,$$

$$\mathcal{B}(D^0 \to K^-K^+\pi^0) = (0.334 \pm 0.004 \pm 0.006 \pm 0.012)\%,$$

Belle

$$\mathcal{B}(D^0 \to \pi^-\pi^+\pi^0) = (1.369 \pm 0.013 \pm 0.042 \pm 0.049)\%,$$

where the errors are statistical, systematic, and due to the uncertainty of $\mathcal{B}(D^0 \to K^-\pi^+\pi^0)$.

The decay rate for each process can be written as:

$$\Gamma = \int d\Phi |\mathcal{M}|^2,$$

where Γ is the decay rate to a particular three-body final state, $\mathcal{M}$ is the decay matrix element, and Φ is the phase space. Integrating over the Dalitz plot

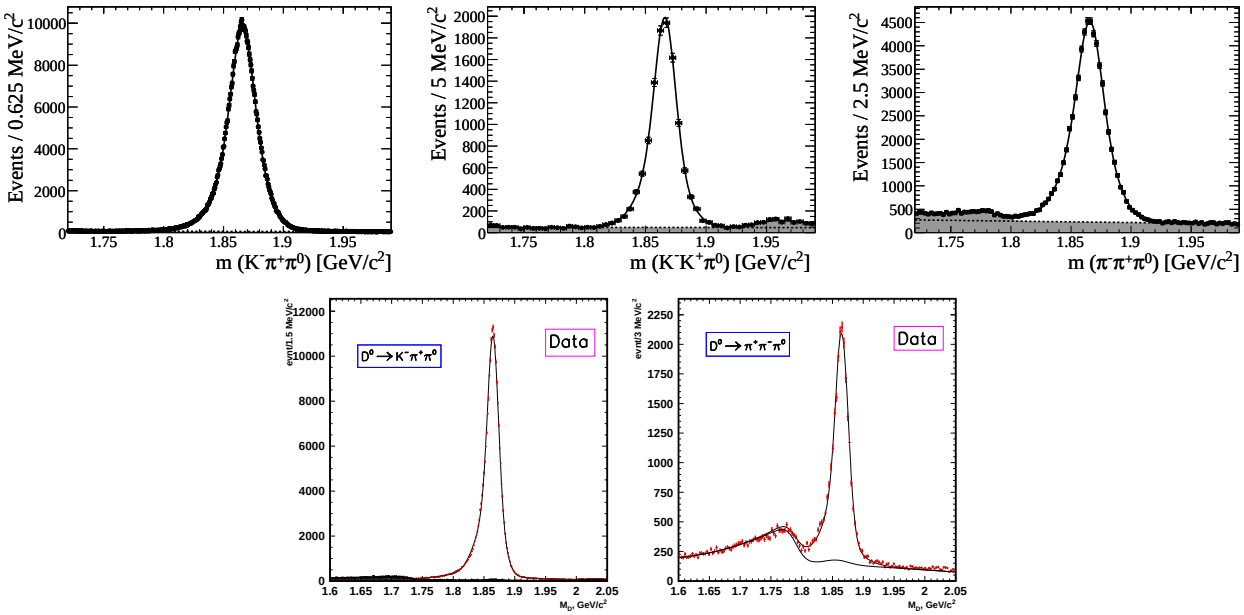

Figure 3: *Top*(*BABAR* collaboration): Fitted mass for the $K^-\pi^+\pi^0$, $\pi^-\pi^+\pi^0$, and $K^-K^+\pi^0$ data samples. Dots are data points and the solid curves are the fit. The dot-dashed lines show the level of combinatorial background in each case. For the $\pi^-\pi^+\pi^0$ and the $K^-K^+\pi^0$ modes, the shaded region represents the total background. *Bottom*(Belle collaboration): Signal $M(K\pi\pi^0)$ distribution fitted with 2 bifurcated Gaussians + Gaussian (signal peak) and the generic MC shape (background). Signal $M(\pi^+\pi^-\pi^0)$ distribution, fitted to the signal MC shape for the signal peak and with the generic MC shape (background).

assuming a uniform phase space density, the above equation can be written as:

$$\Gamma = \langle|\mathcal{M}|^2\rangle \times \Phi,$$

where $\langle|\mathcal{M}|^2\rangle$ is the average value of $|\mathcal{M}|^2$ over the Dalitz plot and the three-body phase space, Φ is proportional to the area of the Dalitz plot. For the three signal decays Φ is in the ratio $\pi^-\pi^+\pi^0 : K^-\pi^+\pi^0 : K^-K^+\pi^0 = 5.05 : 3.19 : 1.67$. Combining the statistical and systematic errors, it results:

BABAR

$$\frac{\langle|\mathcal{M}|^2\rangle(D^0 \to \pi^-\pi^+\pi^0)}{\langle|\mathcal{M}|^2\rangle(D^0 \to K^-\pi^+\pi^0)} = (6.68 \pm 0.04 \pm 0.08)\% \quad (2)$$

$$\frac{\langle|\mathcal{M}|^2\rangle(D^0 \to K^-K^+\pi^0)}{\langle|\mathcal{M}|^2\rangle(D^0 \to K^-\pi^+\pi^0)} = (4.53 \pm 0.06 \pm 0.08)\% \quad (3)$$

$$\frac{\langle|\mathcal{M}|^2\rangle(D^0 \to K^-K^+\pi^0)}{\langle|\mathcal{M}|^2\rangle(D^0 \to \pi^-\pi^+\pi^0)} = (6.78 \pm 0.14 \pm 0.21)\% \quad (4)$$

Belle

$$\frac{\langle|\mathcal{M}|^2\rangle(D^0 \to \pi^-\pi^+\pi^0)}{\langle|\mathcal{M}|^2\rangle(D^0 \to K^-\pi^+\pi^0)} = (6.13 \pm 0.06 \pm 0.19)\% \quad (5)$$

To the extent that the differences in the matrix elements are only due to Cabibbo-suppression at the quark level, the ratios of the matrix elements squared for singly Cabibbo-suppressed decays to that for the Cabibbo-favored decay should be approximately $\sin^2\theta_C \approx 0.05$ and the ratio of the matrix elements squared for the two singly Cabibbo-suppressed decays should be unity. The deviations from this naive picture are less than 35% for these three-body decays. In contrast, the corresponding ratios may be calculated for the two-body decays $D^0 \to \pi^-\pi^+$, $D^0 \to K^-\pi^+$, and $D^0 \to K^-K^+$. Using the world average values for two-body branching ratios [3], the ratios of the matrix elements squared for two-body Cabibbo-suppressed decays, corresponding to Eqs. 2–5, are, respectively, 0.034 ± 0.001, 0.111 ± 0.002, and 3.53 ± 0.12. Thus the naive Cabibbo-suppression model works well for three-body decays but not so well for two-body decays.

5. Amplitude analysis of D and D_s decays

The Dalitz plot analysis is the most complete method of studying the dynamics of three-body charm decays. These decays are expected to proceed through intermediate quasi-two-body modes [9] and experi-

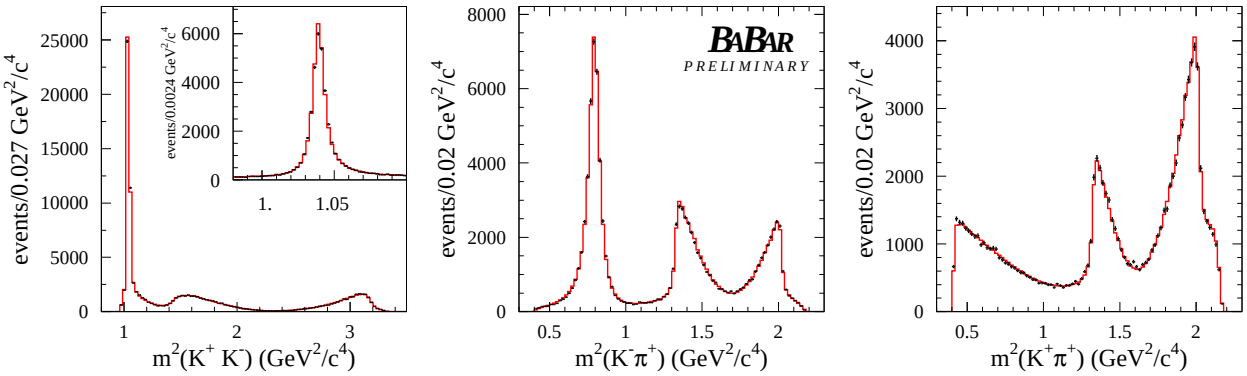

Figure 4: The $D^+ \to K^+K^-\pi^+$ Dalitz plot projections. The data are represented by the points with error bars; the solid histograms are the projections of the fit described in the text. The inset shows an expanded view of the $\phi(1020)$ region.

mentally this is the observed pattern. Dalitz plot analyses can also provide new information on the resonances that contribute to observed three-body final states. In this kind of analysis the complex quantum mechanical amplitude f is a coherent sum of all relevant quasi-two-body $D^0 \to (r \to AB)C$ isobar model [10] resonances, $f = \sum_r a_r e^{i\phi_r} A_r(s)$. Here $s = m^2_{AB}$, and A_r is the resonance amplitude. The isobar model is expected to fail when there are large and overlapping resonances. In such case the $\pi\pi$ S-wave is often parameterized through a K-matrix formalism [11, 12].

5.1. $D_s^+ \to K^+K^-\pi^+$ Dalitz plot analysis

BABAR collaboration reports the study of the three-body D_s^+ meson decays to K^+ K^- π^+ and in particular the measurement of the branching fractions $\frac{\mathcal{B}(D_s^+\to\phi\pi^+)}{\mathcal{B}(D_s^+\to K^+K^-\pi^+)}$ and $\frac{\mathcal{B}(D_s^+\to\overline{K}^{*0}K^-)}{\mathcal{B}(D_s^+\to K^+K^-\pi^+)}$. The decay $D_s^+ \to \phi\pi^+$ is frequently used in particle physics as the D_s^+ reference decay mode. The improvement in the measurements of these ratios is therefore important because it allows the $D_s^+ \to K^+$ K^- π^+ to be used as reference.

A sample of 101k events with a purity of 95% is selected by a likelihood function using vertex separation and p^*, the momentum of D_s^+ in CM system. A 66% of this final sample consists of D_s^+'s originating from $D_s^*(2112)^+ \to D_s^+\gamma$ decay where the variable

$$\Delta m = m(K^+K^-\pi^+\gamma) - m(K^+K^-\pi^+)$$

is required to be within $\pm 2\sigma$ of the PDG value [3].

The selection efficiency is determined from a sample of Monte-Carlo events in which the D_s^+ decay is generated according to phase-space.

An unbinned maximum likelihood fit is performed in order to use the distribution of events in the Dalitz plot to determine the relative amplitudes and phases of intermediate resonant and non-resonant states.

The best fit results showing fractions, are summarized in Tab. II. The decay results to be dominated by $K^*(892)$ and ϕ. Their branching ratio are:

$$\frac{\mathcal{B}(D_s^+ \to \phi\pi^+)}{\mathcal{B}(D_s^+ \to K^+K^-\pi^+)} = 0.379 \pm 0.002 \pm 0.018$$

and

$$\frac{\mathcal{B}(D_s^+ \to \bar{K}^*(892)^0K^+)}{\mathcal{B}(D_s^+ \to K^+K^-\pi^+)} = 0.487 \pm 0.002 \pm 0.016$$

where errors are statistic and systematic respectively. These measurements are much more precise than the previous ones, based on a Dalitz plot analysis of only 700 events [13].

A $f_0(890)$ contribution is large but it is affected by large systematic errors as well due to uncertainness on $f_0(980)$ and $f_0(1370)$ parameters. The Dalitz plot projections together with the fit results are shown in Fig. 4.

Table II Fit fractions of a Dalitz plot fit of $D_s^+ \to K^+K^-\pi^+$ decay. Errors are statistical and systematic respectively.

Decay Mode	Decay fraction(%)
$\bar{K}^*(892)^0K^+$	$48.7 \pm 0.2 \pm 1.6$
$\phi(1020)\pi^+$	$37.9 \pm 0.2 \pm 1.8$
$f_0(980)\pi^+$	$35 \pm 1 \pm 14$
$\bar{K}_0^*(1430)^0K^+$	$2.0 \pm 0.2 \pm 3.3$
$f_0(1710)\pi^+$	$2.0 \pm 0.1 \pm 1.0$
$f_0(1370)\pi^+$	$6.3 \pm 0.6 \pm 4.8$
$\bar{K}_2^*(1430)^0K^+$	$0.17 \pm 0.05 \pm 0.3$
$f_2(1270)\pi^+$	$0.18 \pm 0.03 \pm 0.4$

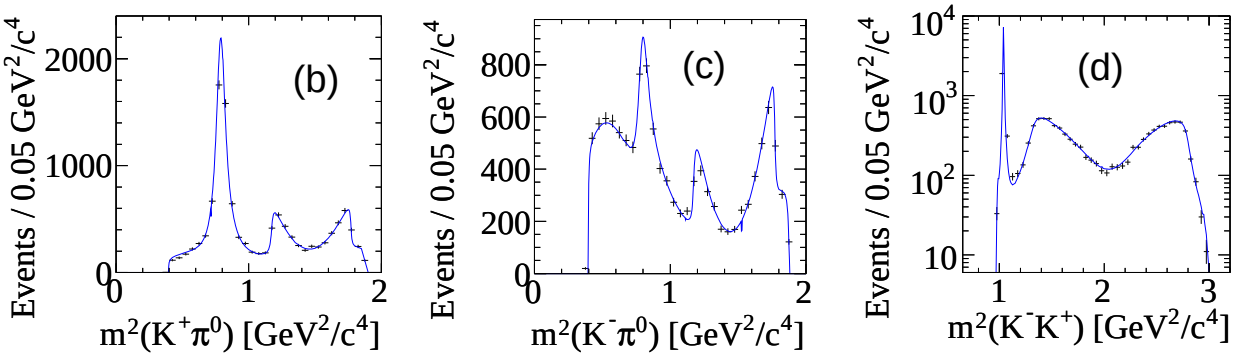

Figure 5: Squared invariant mass projections of $D^0 \to K^-K^+\pi^0$ Dalitz plot. The dots (with error bars, black) are data points and the solid lines (blue) correspond to the isobar fit model.

Further tests of the fit quality are performed using unnormalized Y_L^0 moment projections onto the K^+K^- and $K^-\pi^+$ axis as functions of the helicity angles θ_K and θ_π. For K^+K^-, the angle θ_K is defined as the angle between the K^- for D_s^+ (or K^+ for D_s^-) in the K^+K^- rest frame and the K^+K^- direction in the D_s^+ rest frame. The K^+K^- mass distribution is then modified by weighting by the spherical harmonic $Y_L^0(\cos\theta_K)$ (L=1–4). A similar procedure is followed for the $K^-\pi^+$ system. The resulting $\langle Y_1^0 \rangle$ distributions are shown in Fig. 6.

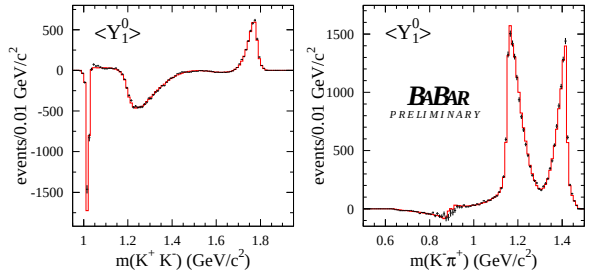

Figure 6: The unnormalized spherical harmonic moments $\langle Y_1^0 \rangle$ as a function of K^+K^- and $K^-\pi^+$ effective masses. The data are presented with error bars, the solid histograms represents the fit projections.

In order to interpret these distributions, one should recall the relationship between $\langle Y_1^0 \rangle$ moments and S- and P-wave amplitudes [14]:

$$\sqrt{4\pi}\,\langle Y_1^0 \rangle = 2 \mid S \mid\mid P \mid \cos\phi_{SP} \qquad (6)$$

Here S and P are proportional to the size of the S- and P-wave contributions and ϕ_{SP} is their relative phase. So $\langle Y_1^0 \rangle$ results to be related to the S-P interference. Due to the presence of strong reflections on the K^+K^- channel from the $K^-\pi^+$ channel (and vice versa), Eq. 6 is meaningful only in the threshold regions. Figure 6 shows a large activity in the low K^+K^- mass distribution, suggesting the presence of a large S-wave contribution below the $\phi(1020)$. The $\langle Y_1^0 \rangle$ distribution along the $K^-\pi^+$ projection, on the other hand, has a very small activity in the $\bar{K}^*(892)^0$, suggesting a small $K\pi$ S-wave contribution.

5.2. $D^0 \to K^+K^-\pi^0$ Dalitz plot analysis

The $K^\pm\pi^0$ systems [15] from the decay $D^0 \to K^-K^+\pi^0$can provide information on the $K\pi$ S-wave amplitude in the mass range 0.6–1.4 GeV/c^2, and hence on the possible existence of the $\kappa(800)$, reported to date only in the neutral state ($\kappa^0 \to K^-\pi^+$) [16]. If the κ has isospin 1/2, it should be observable also in the charged states. Results of the present analysis can also be an input for extracting the CP-violating phase γ [17, 18].

D^0 from $\overline{D}^0$ are identified by reconstructing the decays $D^{*+} \to D^0\pi^+$ and $D^{*-} \to \overline{D}^0\pi^-$. The signal efficiency is estimated for each event as a function of its position in the Dalitz plot using simulated $D^0 \to K^-K^+\pi^0$ events from $c\bar{c}$ decays, generated uniformly in the available phase space.

For D^0 decays to $K^\pm\pi^0$ S-wave states, three amplitude models are considered: the LASS amplitude for $K^-\pi^+ \to K^-\pi^+$ elastic scattering [19], the E-791 results for the $K^-\pi^+$ S-wave amplitude from an energy-independent partial-wave analysis in the decay $D^+ \to K^-\pi^+\pi^+$ [20] and a coherent sum of a uniform nonresonant term, and Breit-Wigner terms for the $\kappa(800)$ and $K_0^*(1430)$ resonances.

The results of an unbinned maximum likelihood are shown in Fig. 5. While the measured fit fraction(Tab. III) for $D^0 \to K^{*+}K^-$ agrees well with a phenomenological prediction [21] based on a large SU(3) symmetry breaking, the corresponding results for $D^0 \to K^{*-}K^+$ and the color-suppressed $D^0 \to \phi\pi^0$ decays differ significantly from the predicted values. The $K\pi$ S-wave amplitude is consistent with that from the LASS analysis, throughout the available mass range. The K^-K^+ S-wave amplitude, parameterized as either $f_0(980)$ or $a_0(980)^0$, is required. No

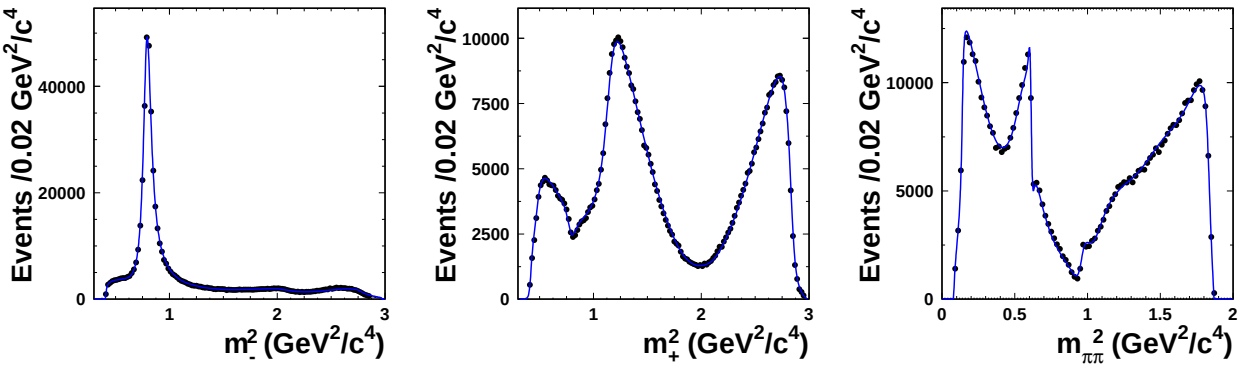

Figure 7: Dalitz plot distribution and the projections for data (points with error bars) and the fit result (curve). Here, $m^2_{\pm}$ corresponds to $m^2(K^0_S\pi^{\pm})$ for D^0 decays and to $m^2(K^0_S\pi^{\mp})$ for $\overline{D}^0$ decays(Belle collaboration).

higher mass f_0 states are found to contribute significantly.

Table III The results obtained from the $D^0 \to K^-K^+\pi^0$ Dalitz plot fit. The errors are statistical and systematic, respectively. The $a_0(980)$ contribution, when it is included in place of the $f_0(980)$, is shown in square brackets. LASS amplitude is used to describe the $K\pi$ S-wave states.

State	Decay fraction(%)
$K^*(892)^+$	$45.2 \pm 0.8 \pm 0.6$
$K^*(1410)^+$	$3.7 \pm 1.1 \pm 1.1$
$K^+\pi^0(S)$	$16.3 \pm 3.4 \pm 2.1$
$\phi(1020)$	$19.3 \pm 0.6 \pm 0.4$
$f_0(980)$	$6.7 \pm 1.4 \pm 1.2$
$\left[a_0(980)^0\right]$	$[6.0 \pm 1.8 \pm 1.2]$
$f_2'(1525)$	$0.08 \pm 0.04 \pm 0.05$
$K^*(892)^-$	$16.0 \pm 0.8 \pm 0.6$
$K^*(1410)^-$	$4.8 \pm 1.8 \pm 1.2$
$K^-\pi^0(S)$	$2.7 \pm 1.4 \pm 0.8$

Neglecting CP violation, the strong phase difference, δ_D, between the $\overline{D}^0$ and D^0 decays to $K^*(892)^+K^-$ state and their amplitude ratio, r_D, are given by

$$r_D e^{i\delta_D} = \frac{a_{D^0\to K^{*-}K^+}}{a_{D^0\to K^{*+}K^-}} e^{i(\delta_{K^{*-}K^+} - \delta_{K^{*+}K^-})}.$$

BABAR finds $\delta_D = -35.5^\circ \pm 1.9^\circ$ (stat) $\pm 2.2^\circ$ (syst) and $r_D = 0.599 \pm 0.013$ (stat) $\pm$ 0.011 (syst). These results are consistent with the previous measurements [22], $\delta_D = -28^\circ \pm 8^\circ$ (stat) $\pm 11^\circ$ (syst) and $r_D = 0.52 \pm 0.05$ (stat) $\pm$ 0.04 (syst).

5.3. $D^0 \to K^0_S\pi^+\pi^-$ Dalitz plot analysis

Recently, evidence for D^0-$\overline{D}^0$ mixing has been found in $D^0 \to K^+K^-/\pi^+\pi^-$ [24] and $D^0 \to K^+\pi^-$ [25] decays. It is important to measure D^0-$\overline{D}^0$ mixing in other decay modes and to search for CP-violating effects in order to determine whether physics contributions outside the SM are present. Belle [23] collaboration reports a measurement of D^0-$\overline{D}^0$ mixing studying $D^0 \to K^0_S\pi^+\pi^-$ decay. The relevance of this decay is enhanced by its role in determining the angle $\gamma \equiv \arg\left[-V_{ud}V^*_{ub}/V_{cd}V^*_{cb}\right]$ of the Unitarity Triangle. In fact, various methods [28] have been proposed to extract γ using $B^- \to \tilde{D}^0K^-$ decays, all exploiting the interference between the color allowed $B^- \to D^0K^-$ ($\propto V_{cb}$) and the color suppressed $B^- \to \overline{D}^0K^-$ ($\propto V_{ub}$) transitions, when the D^0 and $\overline{D}^0$ are reconstructed in a common final state. The symbol $\tilde{D}^0$ indicates either a D^0 or a $\overline{D}^0$ meson. Among the $\tilde{D}^0$ decay modes studied so far the $K^0_S\pi^-\pi^+$ channel is the one with the highest sensitivity to γ because of the best overall combination of branching ratio magnitude, $D^0 - \overline{D}^0$ interference and background level. *BABAR* collaboration reports a measurement of the angle γ by studying the Dalitz plot of $D^0 \to K^0_S\pi^+\pi^-$ [27]. In order to estimate the systematic errors due to model, *BABAR* reports a Dalitz plot analysis where the $\pi\pi$ S-wave is parameterized by a K-matrix model [26].

The results of these analyses are summarized in Tab. IV. The decay is dominated by the $K^*(892)^-$ and $\rho(770)$ contribution. In order to improve the quality of fits, doubly Cabibbo suppressed K^* contributions and two Breit-Wigner amplitudes σ_1 and σ_2 (whose masses and widths are float parameters) are included. σ_1 and σ_2 take in account the poor knowledge of S-wave in the low mass spectrum and $f_0(980)$ parameters. The K-matrix model overcomes this problem describing the $\pi\pi$ S-wave at all.

Figure 7 shows the results of unbinned maximum likelihood fit performed by Belle [23].

Table IV Summary of branching ratios of $D^0 \to K^0_S\pi^+\pi^-$ Dalitz plot fits performed by Belle(Isobar Model) and *BABAR*(Isobar and K-matrix Model).

	Belle	BaBar	
	Isobar Model	Isobar Model	K-matrix Model
State	Fit Fraction(%)		
$K^*(892)^-$	62.27	58.1	58.9
$K^*_0(1430)^-$	7.24	6.7	9.1
$K^*_2(1430)^-$	1.33	3.6	3.1
$K^*(1410)^-$	0.48	0.1	0.2
$K^*(1680)^-$	0.02	0.6	1.4
$K^*(892)^+$	0.54	0.5	0.7
$K^*_0(1430)^+$	0.47	0.0	0.2
$K^*_2(1430)^+$	0.13	0.1	0.0
$K^*(1410)^+$	0.13	—	—
$K^*(1680)^+$	0.04	—	—
$\rho(770)$	21.11	21.6	22.3
$\omega(782)$	0.63	0.7	0.6
$f_2(1270)$	1.8	2.1	2.7
$\rho(1450)$	0.24	0.1	0.3
$f_0(980)$	4.52	6.4	
$f_0(1370)$	1.62	2.0	S-wave
σ_1	9.14	7.6	16.2
σ_2	0.88	0.9	
NR	6.15	8.5	

Acknowledgments

We are grateful for the extraordinary contributions of our PEP-II colleagues in achieving the excellent luminosity and machine conditions that have made this work possible. The success of this project also relies critically on the expertise and dedication of the computing organizations that support *BABAR*. The collaborating institutions wish to thank SLAC for its support and the kind hospitality extended to them. This work is supported by the US Department of Energy and National Science Foundation, the Natural Sciences and Engineering Research Council (Canada), the Commissariat à l'Energie Atomique and Institut National de Physique Nucléaire et de Physique des Particules (France), the Bundesministerium für Bildung und Forschung and Deutsche Forschungsgemeinschaft (Germany), the Istituto Nazionale di Fisica Nucleare (Italy), the Foundation for Fundamental Research on Matter (The Netherlands), the Research Council of Norway, the Ministry of Education and Science of the Russian Federation, Ministerio de Educación y Ciencia (Spain), and the Science and Technology Facilities Council (United Kingdom). Individuals have received support from the Marie-Curie IEF program (European Union) and the A. P. Sloan Foundation.

References

[1] N. Cabibbo, Phys. Rev. Lett. **10**, 531 (1963); M. Kobayashi and T. Maskawa, Prog. Theor. Phys. **49**, 652 (1973).
[2] B. Aubert *et al.* [BABAR Collaboration], arXiv:0704.2080 [hep-ex].
[3] W.-M. Yao *et al.* (Particle Data Group), J. Phys. G **33**, 1 (2006).
[4] F. J. Ronga *et al.* (Belle collaboration), Phys. Rev. D **73**, 092003 (2006).
[5] B. Aubert *et al.* (BaBar collaboration), Phys. Rev. D **71**, 112003 (2005).
[6] K. Abe *et al.* [Belle Collaboration], arXiv:hep-ex/0701053.
[7] B. Aubert *et al.* [BABAR Collaboration], Phys. Rev. D **74**, 111103 (2006).
[8] K. Abe *et al.* [BELLE Collaboration], arXiv:hep-ex/0610062.
[9] M. Bauer *et al.*, Z. Phys. **C34**, 103 (1987).
[10] S.J. Lindenbaum and R.M. Sternheimer, Phys. Rev. **105**, 1874 (1957); M.G. Olsson and G.V. Yodh, Phys. Rev. **145**, 1309 (1966); D.J. Herndon, P. Söding, and R.J. Cashmore, Phys. Rev. **D11**, 3165 (1975).
[11] E. P. Wigner, Phys. Rev. 70 (1946) 15; S. U. Chung *et al.*, Ann. Physik 4 (1995) 404.
[12] I. J. R. Aitchison, Nucl. Phys. **A189**, 417 (1972).
[13] E687 Collaboration, P.L. Frabetti et al., Phys. Lett. **B351**, 591 (1995).
[14] S.U. Chung, Phys. Rev. **D56**, 7299 (1997).
[15] B. Aubert *et al.* [BABAR Collaboration], Phys. Rev. D **76**, 011102 (2007).
[16] E.M. Aitala *et al.* (E-791), Phys. Rev. Lett. **89**, 121801 (2002).
[17] A. Giri, Y. Grossman, A. Soffer, and J. Zupan, Phys. Rev. **D68**, 054018 (2003).
[18] B. Aubert *et al.* (*BABAR*), hep-ex/0703037, submitted to Phys. Rev. Lett.
[19] D. Aston *et al.* (LASS), Nucl. Phys. **B296**, 493 (1988).
[20] E.M. Aitala *et al.* (E-791), Phys. Rev. **D73**, 032004 (2006).
[21] F. Buccella *et al.*, Phys. Rev. **D51**, 3478 (1995).
[22] C. Cawlfield *et al.* (CLEO), Phys. Rev. **D74**, 031108 (2006).
[23] K. Abe *et al.* [BELLE Collaboration], arXiv:0704.1000 [hep-ex].
[24] M. Starič *et al.* (Belle Collaboration), Phys. Rev. Lett. **98**, 211803 (2007).
[25] B. Aubert *et al.* (BaBar Collaboration), Phys. Rev. Lett. **98**, 211802 (2007).
[26] B. Aubert *et al.* [BABAR Collaboration], arXiv:hep-ex/0507101.
[27] B. Aubert *et al.* [BABAR Collaboration], arXiv:hep-ex/0607104.
[28] A. Giri, Yu. Grossman, A. Soffer and J. Zupan, Phys. Rev. D **68**, 054018 (2003).